ESPLANADE: Efficient Simulation of Plasmonic Logic and Arithmetic NAnoDEvice

Manvendra Janmaijaya, Cheikh Brahim El Vaigh, Nicolas Gros, Aurélie Bertaux, Ouassila Narsis Labbani, Sandeep Kumar, Gérard Colas Des Francs, Alexandre Bouhelier, Christophe Nicolle, Erik Dujardin

ESPLANADE: Efficient Simulation of Plasmonic Logic and Arithmetic NAnoDEvice

Manvendra Janmaijaya *,Cheikh Brahim El Vaigh*, Nicolas Gros*, Aurélie Bertaux*, Ouassila Labbani Narsis*, Sandeep Kumar*, Gérard Colas des Francs †, Alexandre Bouhelier†, Christophe Nicolle* and Erik Dujardin †
*CIAD UR 7533, Université Bourgogne Europe, Dijon, F-21000, France
†Laboratoire Interdisciplinaire Carnot de Bourgogne, CNRS UMR 6303, Université Bourgogne Europe, Dijon, 21000, France

***Abstract*—As traditional semiconductor-based computing is approaching its physical limits, plasmonics emerge as a promising alternative, offering the possibility of ultra-compact and high-speed devices. However, plasmonic logic gates suffer from a complex interplay of various parameters such as geometry, material properties, and incident light characteristics. This paper proposes a Genetic Algorithm (GA) termed Efficient Simulation of Plasmonic Logic and Arithmetic Nano Device (ESPLANADE) to optimize these parameters for designing highly efficient plasmonic Arithmetic and Logical Unit (ALU). An efficient procedure with the pyGDM toolkit is used to simulate the electromagnetic interactions, reducing the simulation time. Thorough experiments are conducted to rigorously analyze the performance of ESPLANADE in designing a 1-bit adder, showing its effectiveness and efficiency.**

***Index Terms*—Plasmonic, Logic Gates, Full Adder, Genetic Algorithm, Green Dyadic Method.**

I. Introduction

In the relentless quest for computational efficiency and performance, exploring alternative computing paradigms has become increasingly crucial as traditional electronic computing approaches its physical and practical limits, including size, speed, and heat. Optical computing leverages the properties of light for the development of high-speed and low-dissipation computational devices. Plasmonics exploits the interaction of light with free electrons in metal nanostructures and offers new ways of manipulating and processing information at the nanoscale. At the heart of plasmonic computing are all-optical logic gates, which perform logical operations using light. These gates are the foundational elements of the photonic Arithmetic and Logic Unit (ALU), executing arithmetic and logical functions essential for computational tasks [23], [24].

Physicists study plasmonic logic gates as an alternative to semiconducting transistors in computing. They are achieved by linear interference mechanisms or non-linear optical effects such as the Kerr effect and four-wave mixing [16]. The core idea in designing plasmonic logic gates relies upon optimizing constructive or destructive interference in two or more plasmonic waveguides. While this approach demonstrates the feasibility of plasmonic logic gates, a fully operational computing paradigm using these technologies is yet to be demonstrated.

The output of plasmonic logic gates depends on a complex interplay between several parameters, among which the device geometry, the plasmonic properties of the chosen material, and the incident light characteristics. One recent approach consists in focusing laser beams onto specific input locations of a flat gold structure having a double hexagonal (DH) shape shown in Figure 1. Upon light excitation, the structure generates remotely another light signal that constitutes the device output response. One laser beam feature (e.g., polarization) encodes the Boolean input. A logic function is achieved by the device if the relationship between the output signal and the input configuration follows the truth table of the logic function. However, given a desired logic gate, it is extremely complex to determine all the parameters for which the logic function is actually performed. For example, in the DH case, if one considers a realistically limited parameter space, there are 20 possible inputs locations Figure 1a), 36 possible polarization values (from 0° to 360° by 10° steps) to encode one Boolean input and 36 possible phase shift between the two inputs. One can, therefore, estimate the number of possible configurations for a fixed inputs position to 36x35x36, i.e., 45360 (See Equation 6 in Section III-A). Therefore, it is important to develop an efficient optimization mechanism to find the correct combination of these parameters to get the optimum output. In Figure 1b-1d, such an optimum is shown for an AND gate.

Simulation is performed by the pyGDM python toolkit that employs the Green Dyadic Method (GDM) to obtain electro dynamical simulations of nanostructures [2], [13]. This pyGDM toolkit takes around two hours for one simulation. Finding the best configuration in a brute-force setup will take more than 2992 years for one device! (See Equation 6 in Section III-A). The primary purpose of this work is to search for the optimal solution in the parameter space of the device configurations. We are looking for automatically determining the optimal locations of input lasers and their associated polarizations and phases to encode all logic gates in a given plasmonic device.

Genetic algorithms (GAs) stand as a powerful optimization tool in computational intelligence, drawing inspiration from the principles of natural selection and genetics. Their versatility and robustness make them applicable across various fields, including engineering design, financial modeling, artificial intelligence (AI), and bioinformatics. By efficiently navigating complex and multidimensional search spaces, GAs can find optimal solutions to problems that are otherwise intractable using traditional optimization methods. The core strength of GAs lies in their ability to adapt and evolve solutions over

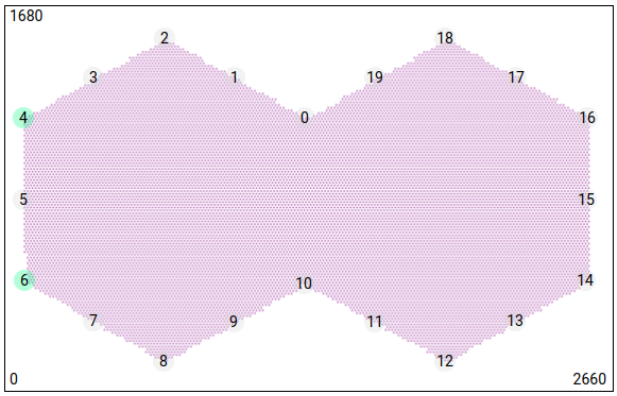

(a) Input lasers positions

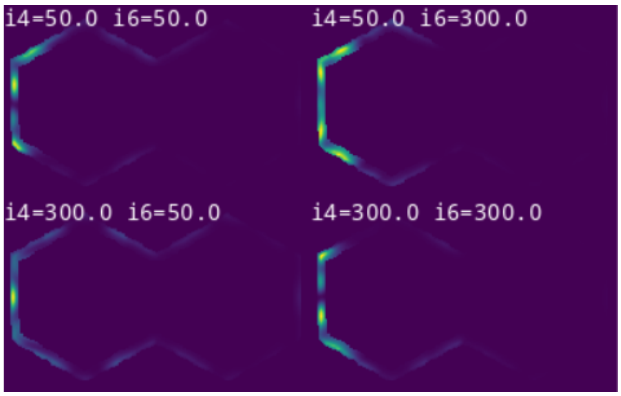

(b) The four different options for two bits inputs

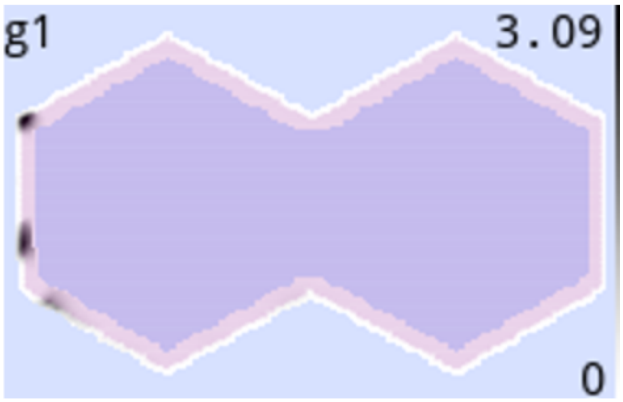

(c) The output near-field g1 measured using Equation 1 as we will explain in Sec III-A

i4	i6	g1
0	0	0
0	1	0
1	0	0
1	1	1

(d) The truth table for AND gate

Fig. 1: A double hexagon (DH) device crafted from 2D crystalline gold, serving as logic gates encoder. Two laser beams, each possessing distinct linear polarizations to encode Boolean inputs ”0” and ”1”, stimulate the device. Inputs i_4 and i_6 are subjected to two laser excitations, showcasing input polarizations of 50° encoding Boolean ”0” and 300° encoding Boolean ”1”. DH device shows a non-zero output as g_1 only in the configuration $i_4 = i_6 = 300°$.

generations, making them particularly suited for optimizing the position, dimension, and geometry of plasmonic structures in the design of plasmonic logic gates.

This paper uses GA to find the optimal parameters allowing the best encoding for a one-bit adder in the double hexagon device.

The main contributions of the paper can be summarized as follows:

1) We designed mathematical optimizations to simulate all logic gates;
2) We implemented an updated version of pyGDM where the electrodynamic simulation time is significantly reduced to approximately 3 ms by precomputing and saving the Dyson equation (propagator matrix). This approach allows us to trade computation time for fast access to memory, avoiding redundant calculations when the propagator i.e, the device shape, remains unchanged across multiple simulations.
3) We proposed a novel generic framework to find the optimal parameters for designing plasmonic logic gates based on genetic algorithms. We optimize for a plasmonic device, simultaneously the input positions of the lasers, their polarization, and phases to encode all logic gates. We term this algorithm ESPLANADE: Efficient Simulation of Plasmonic Logic and Arithmetic NAnoDEvice.
4) An experimental validation of the proposed genetic algorithm provided the best setup to encode a 1-bit adder for different input devices, validating the methodology across diverse geometries.

The rest of the paper is organized as follows: Related works are summarized in Sec. II, Proposed methodology is elaborated in Section III, Sec. IV describes experiment results. In the end, Sec. V is the conclusion.

II. Related Work

This section summarizes the field of designing logic gates using AI. Initially, published work in designing logic gates is summarized in Sec. II-A, then the AI-based logic gates optimization models are reviewed in Sec. II-B.

A. Design of Logic Gates

Logic gates using integrated circuits are fundamental building blocks of digital electronics, performing logical operations

on binary inputs to produce binary outputs within a single semiconductor chip. However, heat dissipation is a severe spoiler in these traditional integrated circuits [25], and physical limitations impact the density of logic gates on chips [26]. An alternative approach to these electronic logic gates is the optical logic gates, which employ lights instead of electric current to perform logic operations. Optical logic gates have a high speed and low power consumption and are built using optical phenomena such as interference, diffraction, or polarization [27]–[29]. Furthermore, logic gates are difficult to integrate into electronic systems, which limits their widespread adoption. They are also not compact, and their manufacture is often more complex and expensive than that of their electronic counterparts [25]–[27]. Finally, plasmonic logic gates combine the benefits of electronic and optical logic gates by leveraging surface plasmon polaritons—electromagnetic waves propagating along the conductor-dielectric interface—operating seamlessly at the nanoscale for highly compact designs [30]–[32]. Nevertheless, designing plasmonic logic gates is influenced by an intricate interplay of multiple factors, including geometry, material attributes, and the properties of incident light.

Several works try to design different plasmonic logic gates [4], [14], [15], [22], [33]–[37]. Al-Musawi et al. [4] proposed a four nanorings and three slots architecture through a dielectric-metal-dielectric plasmonic waveguide to generate logic gates. Yao et al. [36] proposed a quasi-rhombus-shaped structure to manipulate dielectric-loaded waveguides to obtain logic gates by employing destructive and constructive interferences. Amiri et al. [37] proposed a plasmonic-based two-dimensional triangular structure with six air holes drilled in a regular design with copper-based material to obtain plasmonic logic gates. They provided suitable quantification for values of the diameter of air holes and lattice constant in plasmonic-based triangular structures. Dolatabady and Granpayeh [22] proposed and investigated plasmonic logic gates using plasmonic structures with nanodisk resonators by coupling the output and input waveguides in the resonance frequencies of the nanodisk. Swarnakar et al. [34] proposed half-subtractor and half-adder circuits by employing the linear interference principle in a metal-insulator-metal waveguide. Two Y-shaped power combiners were used to design the structure. Nozhat et al. [14] proposed all-optical NAND and XOR logic gates based on a non-periodic array of gold disk-shaped nanoparticles. They examined how the periodicity and spacing of gold disk-shaped nanoparticles affect localized surface plasmon resonances. Destructive interference, achieved through phase differences among input signals, enables NAND gate creation, depending on polarization, particle geometry, and permittivity. Constructive and destructive interferences result from the difference in signal direction and path length. Huang et al. [12] proposed silicon photonic crystal waveguides and phase-encoded light beams for multifunctional half subtractors and half adders. Logic operations are decided based on output light intensity, while the input digital state '1' and digital state '0' are represented using initial phases of incident light viz. 'π' and '0' respectively.

These approaches heavily rely on serendipitous or limited exploration of search space—all possible parameters for designing plasmonic logic gates: phase, polarization, input laser position—This work proposes a complete guided exploration of all the search space parameters for plasmonic-based devices with the help of AI models such as genetic algorithms.

B. AI Based Logic Gates Optimization

Numerous studies leveraged AI to design logic gates. Fernandes et al. [8] used machine learning (ML) to design all-optical logic gates from a Mach-Zehnder Interferometer by tuning its phase shifts to output a desired logic gate. Estimations of phase shifts are based on the maximization of distance between corresponding outputs of logic level '0' and logic level '1' using regression methods. Instead of exploring the complete range of phase shifts, their approach considered a smaller dataset and used ML to estimate the output of remaining phase shifts. An artificial neural network (ANN) is developed in [38] to predict the propagation characteristics of plasmonic nanostrip and coupled nanostrips transmission lines. Parandin et al. [39] also used ANN to optimize the photonic crystal structure parameters for AND gate only. Anagha et al. [10] presented a review covering logical gate designs using AI and topological photonics. They categorized simultaneous gates, reconfigurable gates, modulation-based gates, data rate-based gates, and reversible gates. Finally, Dan et al. [15] proposed to optimize the distributions of coding metamaterials using NSGA-II (the nondominated sorting genetic algorithm) to improve the logic gates performance.

These prior works have explored the use of AI to model some of the parameters used for the design of logic gates, such as the phase [8], propagation characteristics [38] or the coding metamaterials [15]. The closest approach to our work is [15], which uses a genetic algorithm to enhance the logic gates' performance by optimizing the distributions of coding metamaterials only. We propose in this work a multi-objective genetic algorithm that seeks to optimize *all the parameters* of any plasmonic device to efficiently encode all the logic gates. We will show the effectiveness of our approach using a set of plasmonic devices (see Sec. IV).

III. Proposed Methodology

This section describes the proposed methodology of ESPLANADE in detail. Given a desired logic and/or arithmetic function as a Boolean table of truth, ESPLANADE aims to find the optimal parameters to implement it with the highest possible robustness and readout quality. In particular, ESPLANADE explores and optimizes the planar shape of the device, the optical input and output locations, the laser polarizations encoding the Boolean inputs, and the temporal relationship between the input signals (called time delay or phase shift). It also computes a global figure of merit, called Boolean contrast, that is used as a cost function to be maximized. Figure 2 illustrates the flowchart of the proposed approach for a 2-input XOR logic gate. Our methodology relies on two blocks. The first block (Block I) is devoted to the computation of the electromagnetic response to elementary single-beam excitation at each input location. In block II, we combine these excitations to build up the response of a double-beam

excitation. A genetic algorithm (GA) is applied to this part to determine optimal excitation conditions for achieving a given gate functionality. Practically, in block I, step 1 actuates the input to the model, i.e., the shape, material used, and the lasers. Steps 2 to 4 show the use of the revisited version of the PyGDM toolkit to simulate the electromagnetic response of the nanostructure, taking benefit from the Green's Dyad Method that encodes the optical response of the system, independently of the excitation conditions [42], as detailed in Sec. III-A. Steps 5 to 8 depict the procedure of the genetic algorithm for the optimization of a plasmonic device to encode the logic gates. We further explain this algorithm in Sec III-B.

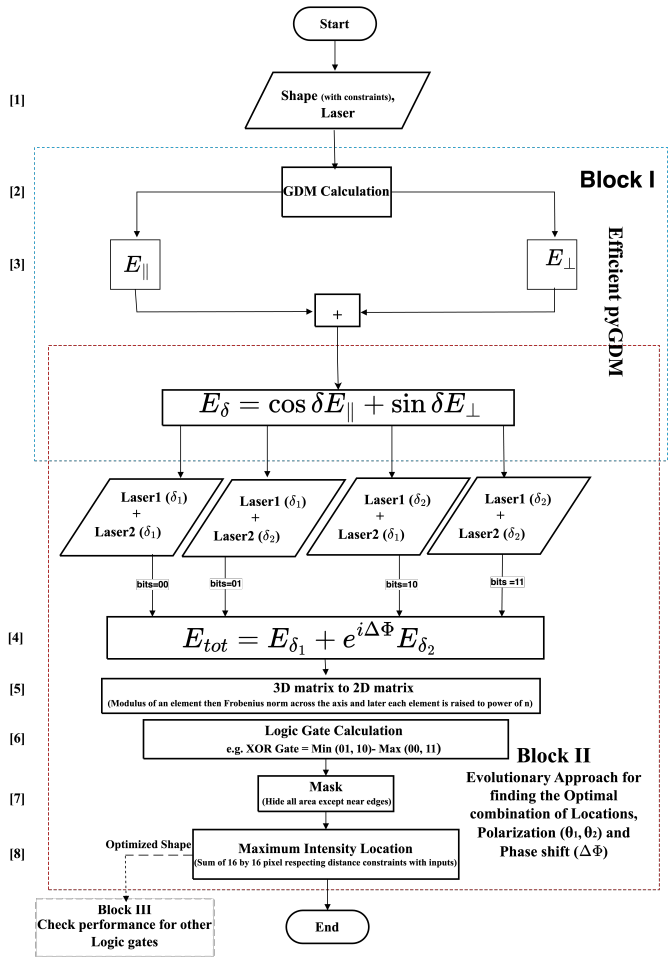

Fig. 2: Flowchart of ESPLANADE algorithm

A. Simulation using PyGDM

PyGDM utilizes Green's Dyadic Method to simulate electromagnetic (EM) interactions within nanostructures [2], [43]. The electromagnetic response of a given nanostructure, at a given angular frequency ω is fully encoded into the Green's tensor $\mathbf{G}$, associated with the structure (shape, material, angular frequency) but does not depend on the excitation conditions (incident field beam positions and polarizations). This particular property is fully exploited in ESPLANADE to strongly reduce the number of computational operations when optimizing the logic and arithmetic nanodevices. We define in step 1 the object shape and material. Then, the optical response for a double beam excitation is obtained in a three-step process as follows: i)

1) Step 2. The Green's dyadic $\mathbf{G}$ associated with the plasmonic device corresponds to the propagation of an electromagnetic signal from point $\mathbf{r}'$ to a point $\mathbf{r}$ and is computed by solving the self-consistent Dyson's equation

$$\mathbf{G}(r,r',\omega) = \mathbf{G}_0(r,r',\omega) + k_0^2 \int_V d^3r''\ \mathbf{G}_0(r,r'',\omega)\cdot[\epsilon_r(\omega)-1]\,\mathbf{G}(r'',r',\omega) \quad (1)$$

Here, $\mathbf{G}_0$ is the Green's dyadic associated with the substrate/air configuration (without the plasmonic nanostructure), $k_0 = \omega/c$ is the wavenumber and $\epsilon_r(\omega)$ refers to the permittivity of the nanostructure at the considered angular frequency. The integration is performed over volume V of the plasmonic structure only. The Green's dyadic has to be computed for numerous position pairs $(\mathbf{r},\mathbf{r}')$ and is saved as a large 3D array of complex numbers. This step is memory-consuming and time-consuming.

2) Step 3: Once Green's dyadic is known, we compute the electric field $\mathbf{E}^n(\mathbf{r}_{obs})$ at the observation points $\mathbf{r}_{obs}$ for an incident field $\mathbf{E}_0$ focused at one of the input positions N. We consider two orthogonal polarizations : 0° ($\mathbf{E}_{0,\parallel}$) and 90° ($\mathbf{E}_{0,\perp}$). The electric field obeys the Lippmann -Schwinger equation (we remove the ω dependency for the sake of clarity)

$$\mathbf{E}^n_{\parallel}(\mathbf{r}_{obs}) = \mathbf{E}^n_{0,\parallel}(\mathbf{r}_{obs}) + k_0^2 \int_V d^3\mathbf{r}''\ \mathbf{r}_{obs},\mathbf{r}'')\cdot[\epsilon_r-1]\,\mathbf{E}^n_{0,\parallel}(\mathbf{r}'') \quad (2)$$

$$\mathbf{E}^n_{\perp}(\mathbf{r}_{obs}) = \mathbf{E}^n_{0,\perp}(\mathbf{r}_{obs}) + k_0^2 \int_V d^3\mathbf{r}''\ \mathbf{G}(\mathbf{r}_{obs},\mathbf{r}'')\cdot[\epsilon_r-1]\,\mathbf{E}^n_{0,\perp}(\mathbf{r}'') \quad (3)$$

Where $n \in [0, N-1]$.
It is worth noticing that $\mathbf{G}$ has to be computed only once (in Step 2) so that Step 3 is efficiently implemented numerically.

3) Step 4. Finally, the excitation response of the two beams is achieved. Consider two incident beams focused at the input ports n_1 and n_2 with polarisation δ_1 and δ_2, respectively. We note $\Delta\Phi$ the phase shift originating from the time delay between the two incident beams. Then, the two beams' response obeys

$$\mathbf{E}_{tot}(\mathbf{r}_{obs}) \quad = \quad \mathbf{E}_{n_1}(\mathbf{r}_{obs}) + \mathbf{E}_{n_2}(\mathbf{r}_{obs})e^{i\Delta\Phi} \quad (4)$$

where the electric field at position $i = n_1, n_2$ for polarization angle δ_i are expressed as a function of the elementary responses Eq. (3)

$$\mathbf{E}_i(\mathbf{r}_{obs}) \quad = \quad \cos\delta_i\ \mathbf{E}^i_{\parallel}(\mathbf{r}_{obs}) + \sin\delta_i\ \mathbf{E}^i_{\perp}(\mathbf{r}_{obs})\ . (5)$$

In particular, we notice that the reconstruction of the two-beam excitation configuration is directly expressed as a function of the elementary parallel and orthogonal single beam excitations at the input ports and the parameters to optimize (input ports, beam polarisations, phase shift). This is very well adapted to a GA optimization, as we will discuss in Section III-B

pyGDM optimization of logic and arithmetic nanodevices could result in huge computational costs. For the N input ports, there are $N(N-1)$ available positions of the two laser inputs. In addition, the phase shift and polarizations are in the range of [0°, 360°[. For a step of 10°, there are 36 different phase shifts and polarizations. So, for two lasers, there are 36×35 combinations of polarizations since each Boolean input is associated with a given polarization. Thus, the total number of combinations for two lasers, including a phase shift, is $36 \times 36 \times 35 = 45360$. Finally, the total time to try all the combinations is

$$C_N(t) = 45360N(N-1)t \tag{6}$$

where t is the time taken by pyGDM for one simulation. For one combination of phase and polarization, pyGDM takes typically $t = 1.5$ hour to simulate the EM response of a plasmonic device of thickness 30 nm and size $2 \times 2\mu m^2$ as the double hexagone of figure 1. For $N = 20$ input ports (see e.g. Figure 1), we achieve $C_{20}(t) = 17,236,800 \times t \approx 3000$ years ! The computation of the Green's dyadic (step 1) is the most time-consuming and computationally expensive part of the simulation, but it can be reused, see Equation (2-3). We can store the computed Green's tensor $\mathbf{G}$ as it remains the same for a given plasmonic device. This permits efficient computation of a given configuration without reconsidering the whole system, as generally done with electromagnetism solvers. For the calculation of the electromagnetic field for a different phase shift, polarizations and input locations, we compute the near-field—the electromagnetic field in the immediate vicinity of nanostructures using Equations 4,5.

Consequentially, we need only to pre-compute the Green's dyadic (step 2) with equation 1 and use equations (3-5) to compute the full two beam electromagnetic response. For example, in the case of the double hexagon structure, it takes one hour and nine minutes (1.15 hours) for step 1 and only 0.005s to realize one simulation using Equations (3-5). The total time for all the combinations based on the new implementation of pyGDM obeys

$$C_N^{opti}(t) = 1.15 + 45360 \times N \times (N-1) \times t \tag{7}$$

And $C_{20}^{opti} = 1.15 + 45360 \times 20 \times 19 \times 0.005/3600 = 25$ hours (about one day). While these two mathematical optimizations (Equation 4 and Equation 5) are well known in the literature, they were not used in the original pyGDM paper [2], and by implementing them, we noticed a huge reduction in the computation time compared to brute force Eq. (6). It reduced the simulation time for the double hexagon from several thousands of years to one day!

B. Parameters Optimization with Genetic Algorithm

In this section, we describe the process for finding the optimal parameters that excite the plasmonic device. In the flow chart (Figure 2), two different lasers are used as inputs to the logic gate in location I_1 and I_2 ($I_1 \neq I_2$) with boolean data encoded with two different polarizations θ_1 and θ_2 ($\theta_1 \neq \theta_2$). Phase of laser incident at location I_1 is α_1 and phase of laser incident at location I_2 is α_2. Since the relative phase is obtained, in practice by time delaying one laser beam with respect to the other one, we assigned a 0° phase to the first beam ($\alpha_1 = 0$), while the phase of the second laser is varied in the range [0, 360[. As mentioned before, the incidence of a laser on the plasmonic device at a particular location outputs a 3D complex matrix using Eq. 1. So, the incidence of two lasers at two different locations on the plasmonic device is simulated by producing two 3D complex matrices using Eq. 2-3 for each laser separately. Keeping the lasers in their I_1 and I_2 locations, four excitation conditions can be generated by changing the beam polarizations. Two lasers with θ_1 (respectively θ_2) polarization encode the 00 (respectively 11) configuration. One laser with θ_1 (respectively θ_2) while the other is polarized with θ_2 (respectively θ_1) encode the 01 (respectively 10) bit configuration. The sum of these two 3-D complex number matrices of the two different lasers produces the response to all Boolean excitation pairs viz. 00, 01,10, 11. The phase of these two lasers remains constant for all polarization combinations. The result of adding two 3D complex number matrices generated by these two lasers using Eq. 4 is also a 3D matrix of complex numbers. These 3D complex number matrices are converted into 2D real numbers by taking the modulus of each element of the matrix, followed by the Frobenius norm (Step 5 of Figure 2). After that, each element of this 2D real number matrix is raised to a power of $n = 3.5$ to obtain the near-field intensity as defined by the squared modulus of the local electric field [41]. These

Algorithm 1 ESPLANADE: Efficient Simulation of Plasmonic Logic and Arithmetic NAnoDEvice

Input: Laser and a Plasmonic Device (e.g. Double Hexagon)
Output: Location, polarization, and phase of the lasers and detected location of logic gates

I **Simulation Setup**
1. Location selection for laser incidence.
2. Pre-compute the Green's Dyadic for the device using: Equation 1

II **Genetic Algorithm for optimization of locations, polarization, and phase of two lasers.**
4. Computation of $\mathbf{E}_{//}, \mathbf{E}_{\perp}$ using Equation 2 and 3
5. Using Equation 5 Construct a 3D matrix simulating the plasmonic device
6. Formulation of inputs of two bits with two lasers as follows:
   i) Bits 00: polarizations are θ_1 and θ_1 respectively.
   ii) Bits 01: polarizations are θ_1, and θ_2 respectively.
   iii) Bits 10: polarizations are θ_2, and θ_1 respectively.
   iv) Bits 11: polarizations are θ_2, and θ_2 respectively.
7. Logic Gate Positioning Map
8. Mask/hide all areas except near edges.
9. Search maximum optical output in a 16×16-pixel location (away from inputs)

operations are shown in Figure 2 in steps 7 and 8. We also summarize our approach in Algorithm 1.

In Step 6, different logic gates are produced using these 2D real number matrices generated for each of the four pairs of binary bits. 00, 01, 10, 11. For the XOR logic gate, the objective function looks for the maximum intensity in the matrix produced by taking the element-wise minimum from the matrix of bits 01 and 10 and subtracting it from the element-wise maximum of the bits 00 and 11 matrices. Indeed, in this situation, there exists a field intensity threshold that is exceeded by the response in configurations 01 and 10 but not in configurations 00 and 11. In such a case, the response follows the Boolean behavior of an XOR gate (which is "1"/true if and only if one of the inputs is "1"/true). To detect an XOR gate in the plasmonic device, we need to maximize the value of O_{XOR} in Equation 8, which ensures that the $min\_element(01, 10)$ is higher than the $max\_element(00, 11)$. All 2-input 1 output logic gate can be associated to similar objective functions as shown in [45] and this general principle can be extended to any Boolean truth table of arbitrary complexity.

$$O_{XOR} = min\_element(01, 10) - max\_element(00, 11) \tag{8}$$

$$O_{AND} = element(11) - max\_element(00, 01, 10) \tag{9}$$

$$O_{OR} = min\_element(01, 10, 11) - element(00) \tag{10}$$

$$O_{NOR} = element(00) - max\_element(01, 10, 11) \tag{11}$$

$$O_{NAND} = min\_element(00, 01, 10) - element(11) \tag{12}$$

$$O_{XNOR} = min\_element(00, 11) - max\_element(01, 10) \tag{13}$$

In step 7, each of the logic gate detection (Equations (10) to Equation. (13)), the area near the boundary of the plasmonic device is inspected to find the location of the highest optical output. In step 8, The maximum optical output is searched near the boundary over 16×16 pixels. Since one pixel is 14nm, a 16×16 pixel area corresponds to a 220×220 nm square, which has a comparable area to the smallest circular zone that can be optically resolved at the considered 810 nm wavelength (called Abbe diffraction limit, 250nm diameter). This corresponds to the minimal area over which the experimental setup will integrate the device's optical response.

TABLE I: Truth table for a 1-bit adder

Input1	Input2	Carry (AND)	Sum (XOR)
0	0	0	0
0	1	0	1
1	0	0	1
1	1	1	0

The algorithm focuses on detecting AND and XOR gates to identify the holistic realization of the 1-bit adder function, the simple arithmetic calculation. Starting from Table I, which depicts the truth table of a one-bit full adder that uses two bits as input and generates simultaneously a carry and a sum as outputs corresponding to the AND gate and XOR gate, respectively. One can notice that optimizing the function *F* in Equation 14 will result in encoding both the AND and XOR gates, which is the same as designing a one-bit full adder. Nevertheless, we can individually optimize any equation from the Equations. (10) to Equation. (13) to detect the corresponding logic gate. Meanwhile, encoding both the AND and XOR gates is enough to detect all the logic gates.

$$F = min(O_{AND}, O_{XOR}) \tag{14}$$

A genetic algorithm is proposed to reduce the simulation time for a plasmonic device. It focuses on designing a one-bit full adder, using *F* as its fitness function. This algorithm follows a classical procedure: it starts with a population of potential solutions encoded as chromosomes. Through successive generations, individuals are selected based on their fitness, undergo crossover to exchange genetic material, and undergo mutation to introduce diversity. These operations continue iteratively until termination criteria are met. This genetic algorithm optimizes for two lasers the selection of parameters, viz. polarization, phase, and location of incidence from a large pool of choices, which otherwise, by brute force, is computationally very expensive and can take several thousand of years!

IV. Experiments

In this section, we describe the experimental setup in detail, including the PyGDM simulation and GA parameters. In addition, we present an experimental simulation of a one-bit adder. Experiments were performed using resources (CPU) from DNUM CCUB (Centre de Calcul de l'Université de Bourgogne.

A. Experimental Setup

The material of the optical structure used for excitation is gold. It is well-known for its excellent chemical inertness and its ability to sustain surface plasmons. This choice of metal is also due to its unique localised surface plasmon resonance characteristics, which can be detected in both the near-infrared and visible regions [14]. These characteristics include strong optical extinction, near-field enhancement, and far-field scattering, which are essential for nanophotonic applications [40].

In our GA, the population size is kept at 500, and the maximum number of generations is set at 50. The dimension of the location variable for a laser incidence is kept equal to the number of locations selected for its incidence at the plasmonic device (20 for the double hexagon). Polarisation and phases are selected in the range [0°, 360°[and [0°, 360°], respectively, with a step of 10 °. We study the optimal parameters of the plasmonic device, i.e., DH, to encode all logic gates for a 1-bit adder in Sect. IV-B

B. Parameters Optimisation

(a) The double hexagon shape

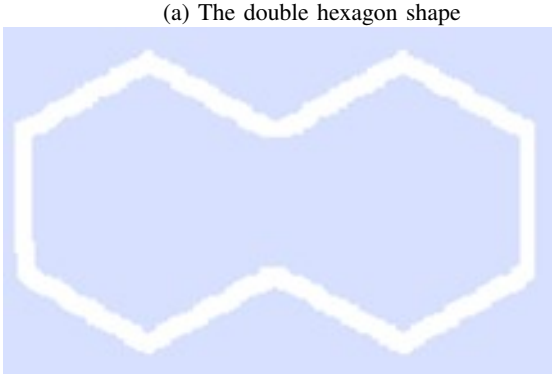

(b) The double hexagon mask

Fig. 3: The double hexagon shape and its associated mask

We first study the double hexagon shape as shown in Figure 3a. In Figure 3b, the boundary of this shape is highlighted. This represents the mask used to direct lasers only in this area, and the output is also observed within this area. For all experiments, the mask comprises an area outside the shape that lies within 14 nm (i.e., one simulation cell size) of the boundary. The mask also includes an area inside the shape up to 55 nm (i.e. the size of 4 simulation cells) inside the boundary. Due to limitations in optical microscope resolution, some constraints are added to physically replicate the experiments to maintain at least 300nm distance between different locations of laser incidence, as depicted in Fig. 4. The radius of the circles shown in the figure is 500nm. Also, outputs are at least 500nm away from inputs and 300nm from other outputs.

A double hexagon-shaped device, when excited with a laser at location 6 as depicted in Fig. 5a, outputs the pyGDM simulation of the excitation as shown in Figure 5b. The polarization of this laser is 280° with respect to horizontal. The result of the excitation is visible in Figure 5b near the position 6.

Similarly, the simulation using two laser configurations is depicted in Figures (6a,6b). Figure 6a depicts the input locations, i.e., lasers are incident at positions 6 and 16. The electromagnetic simulation produced by pyGDM for a double hexagon using four different combinations of these lasers is presented in Figure 6b. These four combinations of lasers are

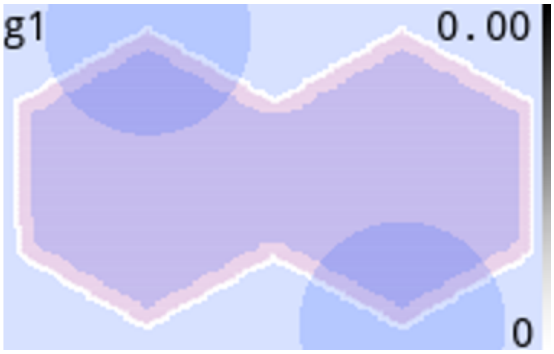

Fig. 4: Distance margin among laser locations and outputs

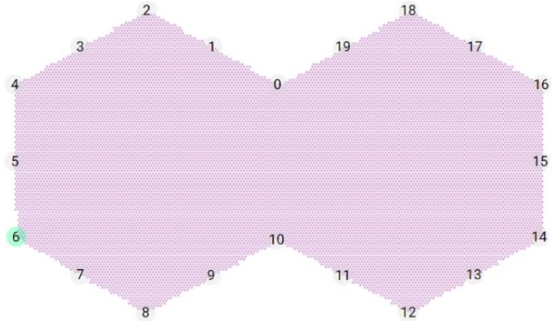

(a) Laser input location at 6

(b) Simulation output

Fig. 5: pyGDM simulation with a laser (phase =0°, polarization = 280°)

generated using two different polarizations of 280.0° and 50.0° at two different locations, 6 and 16. The phase of these lasers is also arbitrarily assigned as 0°.

Figure 6b shows the simulation for both AND and XOR gates. The objective function for these gates is computed using Equations 8-9. For the XOR gate, the location with a maximum detection score (*the sum of the optic output over a 16 × 16 pixel region*) is obtained with a value of 4.12; the region is marked with a square box in Figure 7 (left). For the AND gate, the maximum score is 9.17, and the location of the occurrence of this region is also marked by a rectangular box in Figure 7 (right). A score higher than zero means that we can simulate the logic gate. In Figure 7, we are able to simulate AND and XOR simultaneously in two remote locations of the cavity without any device cascade.

Moreover, Figure 8 depicts another simulation of the DH

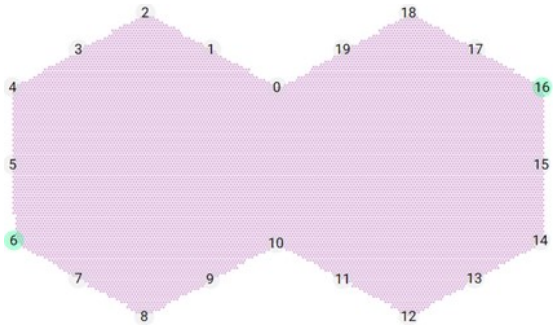

(a) Two Lasers are incident at locations 6 and 16

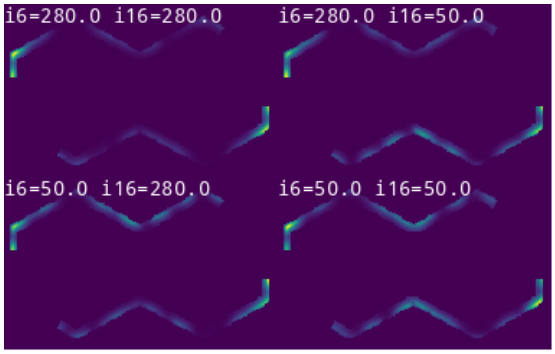

(b) 4 bits simulation using two lasers

Fig. 6: pyGDM simulation with a two lasers (polarization = 50°, polarization = 280°)

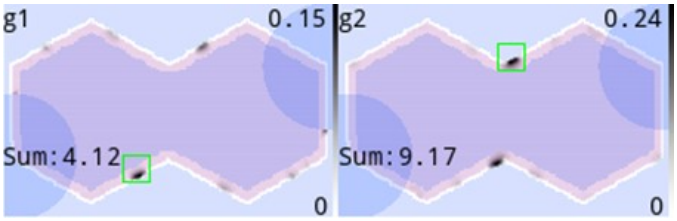

Fig. 7: XOR and AND gate detection with lasers polarization 280° and 50° and phase of 0°. The detection score (Sum) is the some of the optic output over a 16 × 16 pixel region. The value shown in the circle is the near-field. It is 0.15 for the the XOR gate and 0.24 for the AND gate.

when excited with the laser in the second input phase-shifted compared to the first laser by 90°. The input polarizations are 100°(”0”) and 230° (”1”). For the XOR gate, the score is 1.01, and for the AND gate, it is 14.38, as depicted in Figure 9. By changing these parameters (phase and polarization), we noticed that the detection score increased for the AND gate but decreased for the XOR gate. Although the phase is not used to encode the binary input, it plays a crucial role in detecting high-scoring logic gates.

The difference between Figure 7 and Figure 8 illustrates that choosing different input locations or polarization encoding results in significantly different optical responses that can be further tuned with the phase shift to eventually result in different scores for the targeted gates. To identify the XOR gate and AND gates more precisely, it is necessary to maximize the detection scores. The GA is used to simulate

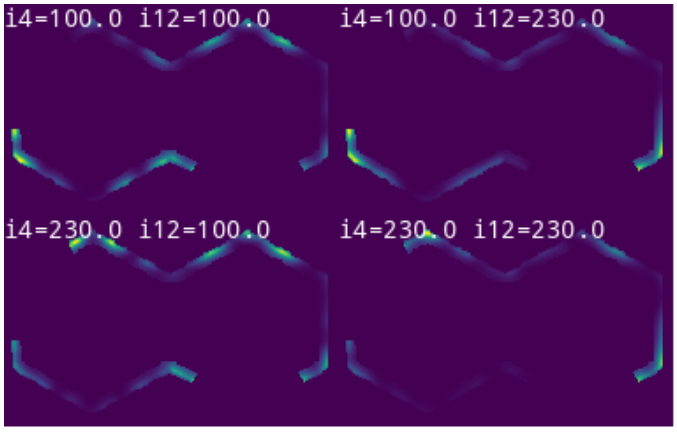

Fig. 8: Two lasers are incident at locations 4 and 12 with the phases 0° and 90° and the polarizations 100 and 230 respectively

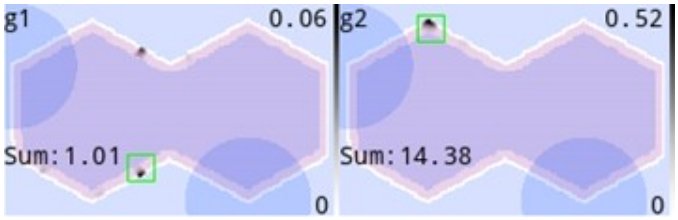

Fig. 9: The detection score for XOR gate (left) and AND gate (right) using non-zero phase

the maximum number of parameters to achieve this objective. For the double hexagon-shaped plasmonic device, the GA obtained optimized results by using locations 13 and 14 for two lasers with phases $\alpha_1 = 0°$ and $\alpha_2 = 120°$, respectively. The polarizations for these lasers are 350° (”0”) and 120° (”1”). The GA optimized the score for both the XOR and AND gates by maximizing the function F in Equation 14. It obtained scores of 77.54 and 78.13 for XOR gate and AND gate, respectively (as shown in Figure 10)

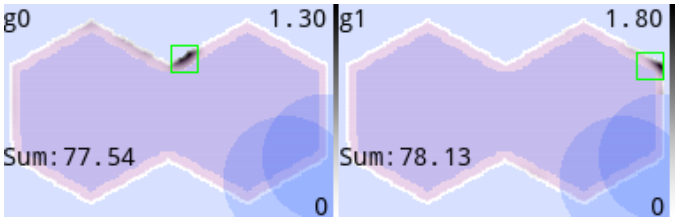

Fig. 10: XOR gate (left) and AND gate (right)

From Figure 7 to Figure 10, it can be seen that using only GA, there is an improvement of at least 640% in the overall score of the 1-bit adder (combined XOR and AND). However, the double hexagon is not an optimized shape of the plasmonic device. Our approach is independent of the double hexagon and can be used with any plasmonic 2D cavity. We further investigate this direction by generating 2D shapes that will better encode the simple logic gates or global table of truth and further maximize their detection scores. More plasmonic devices are presented herein.

Finally, Figure 11 shows the detection of all gates by simply reconfiguring the same double hexagon cavity as demonstrated in [44]. The algorithm first optimizes the concomitant detection of the AND and XOR gates and then looks for all the other gates. We can see in Figure 11 a detection score higher than 0 for all gates. This experimentally proves that detecting AND and XOR gates is enough to detect all logic gates.

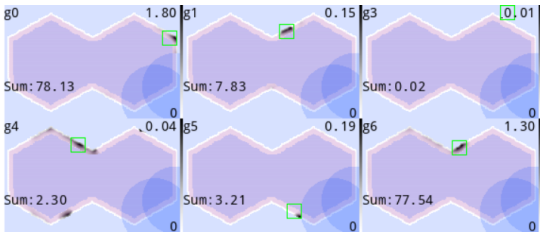

Fig. 11: ALL gates detection in the order: first row(AND, OR, NOT), Second row(NAND, NOR, XOR)

Moreover, to demonstrate the robustness of the model we further investigated different plasmonic shapes in order to optimize logic gates detection scores. We select a set of random points and link them to create a new shape. Figure 12 shows a bow tie form that was created as if two triangles were merged. The Tie device shows a better score than the double hexagon (used here as a baseline). The scores for AND (XOR) are 94.63 (95.70) for the Tie shape and only 77.54 (78.13) for the double hexagon. The detection scores for all logic gates using the Tie device is shown in Figure 13. They are in general better than the ones using the double hexagon.

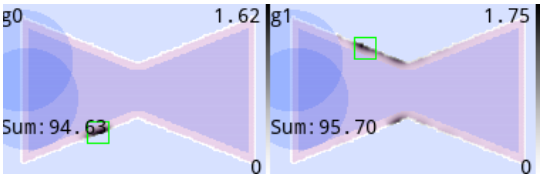

Fig. 12: XOR gate (left) and AND gate (right) for the bow tie

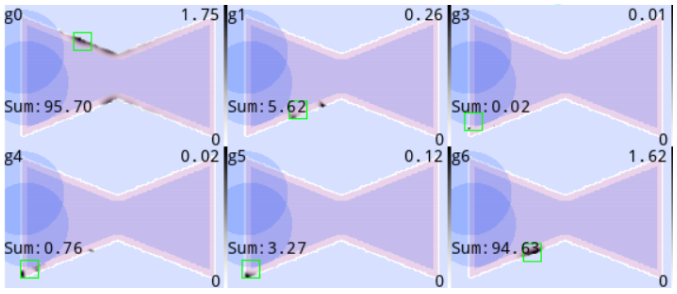

Fig. 13: ALL gates detection with bow tie shape in the order: first row(AND, OR, NOT), Second row(NAND, NOR, XOR)

We studied several shapes, as shown in Figure 14. All the shown figures have a detection score higher than the double hexagon for XOR and AND, and they are all able to encode the different logic gates. Moreover, the Hyena shape gave the highest scores for XOR and AND, showing its superiority with respect to other shapes and particularly the double hexagon.

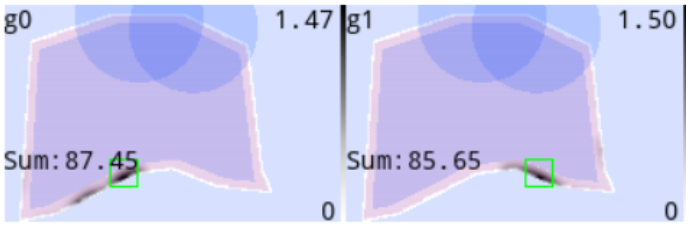

(a) The Book shape

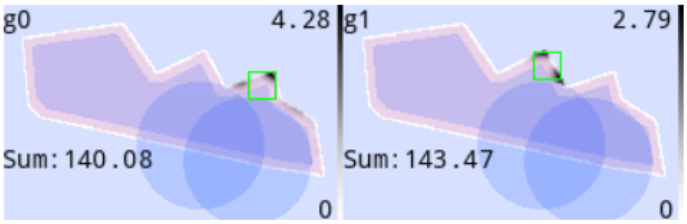

(b) The Titanic shape

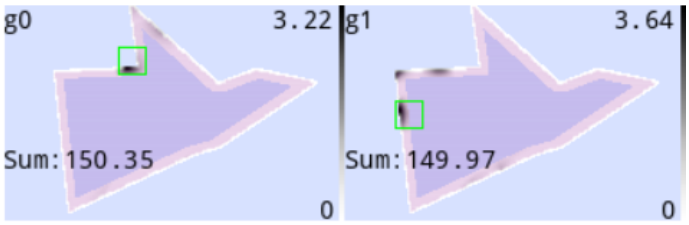

(c) The Hyena shape

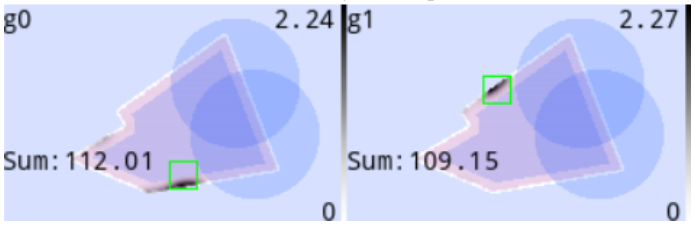

(d) The Mountain shape

Fig. 14: Examples of generated shapes with their XOR and AND scores

Finally, Figure 15 shows the detection scores for all logic gates using the Hyena shape. The logic gates detection scores with the Hyena shape is better than both the bow tie and double hexagon shapes (and all the other shapes). This result suggests that optimizing the results for XOR and AND gates not only allows to detect all logic gates, but higher score for XOR and AND indicates higher scores for all logic gates.

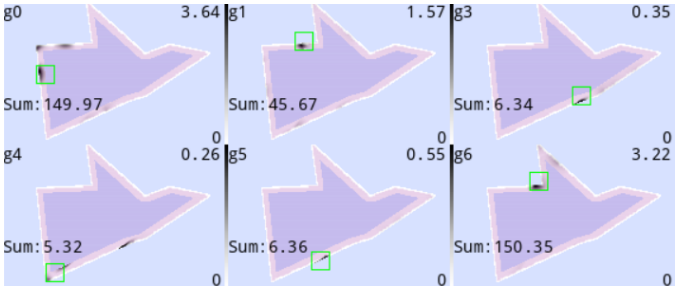

Fig. 15: ALL gates detection with hyena shape in the order: first row(AND, OR, NOT), Second row(NAND, NOR, XOR)

We created a platform based on the proposed algorithm that is available online [1]. This platform was used to produce all the figures of this experimental section and can further be used to reproduce our results, to simulate any logic gates and to explore other complex truth tables using manual exploration or automatic search with GA. More fun shapes that are not presented in this paper can be explored using the platform link.

V. Conclusion

When implementing the concept of holistic plasmonic arithmetic and logic units, the geometry of the plasmonic structure, the location of the lasers, and their phase difference and polarizations have a phenomenal impact on designing plasmonic logic gates using constructive or destructive interference. Arbitrary or intuition-based selection of these parameters may produce sub-optimum results. To address this research gap, this paper proposed a genetic algorithm termed ESPLANADE that optimizes the polarization, phase difference, and location of light incidence.

An efficient pyGDM implementation is proposed to reduce the simulation time from several years to a few days. ESPLANADE uses a GA to simulate a large set of parameters to enhance the detection score of the logic gates.

We experimentally benchmarked ESPLANADE to obtain a 1-bit full adder using two lasers on any device made up of gold material, in line with our recent optical results [44], [45]. ESPLANADE optimized the polarization, phase difference, and location of incidence of the two lasers. This resulted in better detection of plasmonic logic gates by enhancing the detection score by almost 640% over the trial-and-error selection of these parameters.

The proposed approach was validated on the a set of shapes by encoding XOR and AND logic gates to implement a 1-bit adder (available online). As part of future work, we are working on an ontology-based approach for generating efficient 2D shapes that will increase the logic gates detection scores. ESPLANADE is of a generic form, and therefore, it can easily be extended to simulate experiments using four lasers for simultaneous excitation of the structure with 2+2 input ports encoding binary numbers up to 3 to realize a 2-bit Full Adder in a plasmonic cavity able to generate the three required outputs (for a resulting sum value up to 6). Also, ESPLANADE will be modified in the future by using more advanced GA approaches, viz. Non-dominated Sorting Genetic Algorithm -II (NSGA-II), NSGA-III or Generalized Differential Evolution-3 etc.

Acknowledgments

This work has been partially funded by the French Agence Nationale de la Recherche (ANR-20-CE24-0001 DALHAI), the EIPHI Graduate School (ANR-17-EURE-0002) and the Région de Bourgogne Franche-Comté (project Envergure DALHAI-BFC).

[1] https://dalhai.webapp.ciad-lab.fr/

References

[1] Vose, Michael D. The simple genetic algorithm: foundations and theory. MIT press, 1999.

[2] Wiecha, Peter R. "pyGDM—A python toolkit for full-field electrodynamical simulations and evolutionary optimization of nanostructures." Computer Physics Communications 233 (2018): 167-192.

[3] Ozbay, Ekmel. "Plasmonics: merging photonics and electronics at nanoscale dimensions." Science 311, no. 5758 (2006): 189-193.

[4] Al-Musawi, Hassan K., Ali K. Al-Janabi, Salam AW Al-abassi, Noor Al-Huda A. Abusiba, and Noor Al-Huda Q. Al-Fatlawi. "Plasmonic logic gates based on dielectric-metal-dielectric design with two optical communication bands." Optik 223 (2020): 165416.

[5] Wei, Hong, and Hongxing Xu. "Plasmonics in composite nanostructures." Materials Today 17, no.8 (2014): 372-380.

[6] F. Emami, M. Akhlaghi, N. Nozhat, Binary optimization of gold nanorods for designing an optical modulator, J. Comput. Electron. 14 (2015) 574–581.

[7] Zarei, Sanaz, and Amin Khavasi. "Realization of optical logic gates using on-chip diffractive optical neural networks." Scientific Reports 12, no. 1 (2022): 15747.

[8] Fernandes, C. Alexandre R., Manoel EN de Oliveira, Danilo S. Rocha, Auzuir R. de Alexandria, and Glendo F. Guimarães. "Design of Optical Logic Gates Using Mach–Zehnder Interferometers and Machine Learning." Journal of Lightwave Technology 40, no. 18 (2022): 6240-6248.

[9] Masoud, Asmaa M., Ibrahim S. Ahmed, Sahar A. El-Naggar, and Mina D. Asham. "Design and simulation of all-optical logic gates based on two-dimensional photonic crystals." Journal of Optics (2022): 1-9.

[10] Anagha, Erandathara Gokulan, and Ramasamy Kandasamy Jeyachitra. "Review on all-optical logic gates: design techniques and classifications–heading toward high-speed optical integrated circuits." Optical Engineering 61, no. 6 (2022):060902-060902.

[11] Singh, Jeevan Jot, Divya Dhawan, and Neena Gupta. "2D photonic crystal hexagonal ring resonator-based all-optical logic gates." Optics & Laser Technology 165 (2023): 109624.

[12] Huang, Yuhao, Menghang Shi, Aodi Yu, and Li Xia. "Design of multifunctional all-optical logic gates based on photonic crystal waveguides." Applied Optics 62, no. 3 (2023): 774-781.

[13] Wiecha, Peter R., Clément Majorel, Arnaud Arbouet, Adelin Patoux, Yoann Brûlé, Gérard Colas Des Francs, and Christian Girard. "'pyGDM'-new functionalities and major improvements to the python toolkit for nano-optics full-field simulations." Computer Physics Communications 270 (2022):108142.

[14] Nozhat, Najmeh, Hamid Alikomak, and Maryam Khodadadi. "All-optical XOR and NAND logic gates based on plasmonic nanoparticles." Optics Communications 392 (2017): 208-213.

[15] Dan, Yihang, Zeyang Fan, Xiaojuan Sun, Tian Zhang, and Kun Xu. "All-type optical logic gates using plasmonic coding metamaterials and multi-objective optimization." Optics Express 30, no. 7 (2022): 11633-11646.

[16] Wu, Xiaoting, Jinping Tian, and Rongcao Yang. "A type of all-optical logic gate based on graphene surface plasmon polaritons." Optics Communications 403 (2017): 185-192.

[17] Wang, Lujun, Lianshan Yan, Yinghui Guo, Kunhua Wen, Wei Pan, and Bin Luo. "Optical quasi logic gates based on polarization-dependent four-wave mixing in subwavelength metallic waveguides." Optics express 21, no. 12 (2013): 14442-14451.

[18] E. Ringe, J. Zhang, M.R. Langille, K. Sohn, C. Cobley, L. Au, et al., Effect of size, shape, composition, and support film on localized surface plasmon resonance frequency: a single particle approach applied to silver bipyramids and gold and silver nanocubes (MA, United States)Mater. Res. Soc. Symp. Proc. Boston (2009) 52–57.

[19] Girard, Ch, P. R. Wiecha, Aurelien Cuche, and Erik Dujardin. "Designing thermoplasmonic properties of metallic metasurfaces." Journal of Optics 20, no. 7 (2018): 075004.

[20] Wiecha, Peter R., Leo-Jay Black, Yudong Wang, Vincent Paillard, Christian Girard, Otto L. Muskens, and Arnaud Arbouet. "Polarization conversion in plasmonic nanoantennas for metasurfaces using structural asymmetry and mode hybridization." Scientific Reports 7, no. 1 (2017): 40906.

[21] Derkachova, Anastasiya, Krystyna Kolwas, and Iraida Demchenko. "Dielectric function for gold in plasmonics applications: size dependence of plasmon resonance frequencies and damping rates for nanospheres." Plasmonics 11 (2016): 941-951.

[22] Dolatabady, Alireza, and Nosrat Granpayeh. "All optical logic gates based on two dimensional plasmonic waveguides with nanodisk res-

onators." Journal of the Optical Society of Korea 16, no. 4 (2012): 432-442.
[23] Tucker, R.S., 2010. The role of optics in computing. Nature Photonics, 4(7), pp.405-405.
[24] Woods, D. and Naughton, T.J., 2012. Photonic neural networks. Nature Physics, 8(4), pp.257-259.
[25] Arden, W.M., 2002. The international technology roadmap for semiconductors—perspectives and challenges for the next 15 years. Current Opinion in Solid State and Materials Science, 6(5), pp.371-377.
[26] Bandyopadhyay, S., Roychowdhury, V.P. (1996). Granular nanoelectronics. IEEE Potentials.
[27] Jordan, H.F., Heuring, V.P. and Feuerstein, R.O.B.E.R.T., 1994. Optoelectronic time-of-flight design and the demonstration of an all-optical, stored program, digital computer. Proceedings of the IEEE, 82(11), pp.1678-1689.
[28] Kotb, A., Zoiros, K.E. and Li, W., 2023. Silicon-on-silica waveguides-based all-optical logic gates at 1.55 μm. Physica Scripta, 98(3), p.035517.
[29] Kotb, A., Zoiros, K.E. and Guo, C., 2023. All-optical logic gates using E-shaped silicon waveguides at 1.55 μm. Journal of Applied Physics, 133(17).
[30] Al-Sabea, Z.S., Ibrahim, A.A. and Abdulnabi, S.H., 2022. Plasmonic logic gates at optimum optical communications wavelength. Advanced Electromagnetics, 11(4), pp.10-21.
[31] Fakhruldeen, H.F., Mansour, T.S.A., Jabbar, F.I. and Alkhayyat, A., 2022. Multiple inputs all-optical logic gates based on nanoring insulator-metal-insulator plasmonic waveguides. Int. J. Electr. Comput. Eng., 12, pp.6836-6846.
[32] Dan, Y., Fan, Z., Sun, X., Zhang, T. and Xu, K., 2022. All-type optical logic gates using plasmonic coding metamaterials and multi-objective optimization. Optics Express, 30(7), pp.11633-11646.
[33] Mosleh, M., Hamidi, S.M. and Ranjbaran, M., 2022. Multifunctional logic gates based on resonant transmission at atomic-plasmonic structure. Scientific Reports, 12(1), p.10734.
[34] Swarnakar, S., Basha, S.C.A., Azmathullah, S., Prabhu, N.A., Madhu, G. and Kumar, S., 2023. Improved design of all-optical half-adder and half-subtractor circuits using MIM plasmonic waveguides for optical networks. Optical and Quantum Electronics, 55(1), p.94.
[35] Chang, Kai-Hao, Zhan-Hong Lin, Po-Tsung Lee, and Jer-Shing Huang. Enhancing on/off ratio of a dielectric-loaded plasmonic logic gate with an amplitude modulator. Scientific Reports 13, no. 1 (2023): 5020.
[36] Yao, Chaonan, Amer Kotb, Bin Wang, Subhash C. Singh, and Chunlei Guo. All-optical logic gates using dielectric-loaded waveguides with quasi-rhombus metasurfaces. Optics Letters 45, no. 13 (2020): 3769-3772.
[37] Amiri, I. S., G. Palai, S. K. Tripathy, and S. R. Nayak. Realisation of all photonic logic gates using plasmonic-based photonic structure through bandgap analysis. Optik 194 (2019): 163123.
[38] Robert R. Andrawis, Mohamed A. Swillam, Mohamed A. El-Gamal, and Ezzeldin A. Soliman, "Artificial neural network modeling of plasmonic transmission lines," Appl. Opt. 55, 2780-2790 (2016)
[39] Parandin, F., Yahya, S.I., Rezaeenia, M., Askarian, A., Roshani, S., Roshani, S., Ghadi, Y.Y., Jamshidi, M. and Rezaee, S., 2023. A neural networks approach for designing compact all-optical photonic crystal-based AND logic gate. Journal of Optical Communications, (0).
[40] Ghanem, K., Li, Y., Xu, J. and Kan, C., 2023. Recent progress of gold nanostructures and their applications. Physical Chemistry Chemical Physics.
[41] Dell'Ova, F., Brulé, Y., Gros, N., Bizouard, J., Shakirova, D., Bertaux, A., Narsis-Labbani, O., Nicolle, C., des Francs, G.C., Bouhelier, A. and Dujardin, E., 2023. Compact implementation of an all-optical 1-bit full adder by coherent excitation of a single 3-µm2 plasmonic cavity. In EPJ Web of Conferences (Vol. 287, p. 04014). EDP Sciences.
[42] Girard, Christian, "Near fields in nanostructures." Rep. Prog. Phys. 68 (2005) 1883–1933.
[43] Wiecha, Peter R. ""pyGDM" -new functionalities and major improvements to the python toolkit for nano-optics full-field simulations" Computer Physics Communications 270 (2022): 108142.
[44] Kumar, U., Cuche, A., Girard, C., Viarbitskaya, S., Dell'Ova, F., Al Rafrafin, R., and Dujardin, E. Interconnect-Free Multibit Arithmetic and Logic Unit in a Single Reconfigurable 3 $mincrom2$ Plasmonic Cavity. ACS nano, 15(8) (2021), 13351-13359.
[45] Dell'Ova, F., Brûlé, Y., Gros, N., Bizouard, J., Shakirova, D., Bertaux, A., and Dujardin, E. (2024). Compact implementation of a 1-bit adder by coherent 2-beam excitation of a single plasmonic cavity. ACS Photonics, 11(2)(2024), 752-761.

PLACE PHOTO HERE

Manvendra Janmaijaya has submitted his Ph.D. in Computer Science at South Asian University, New Delhi, where his research focused on convolution-based deep learning architectures for temporal and spatio-temporal forecasting. He is currently a Research Assistant at The Alan Turing Institute, London, contributing to the Environment and Sustainability Grand Challenge. He previously worked as a Research Engineer at the University of Burgundy, France, where he developed hybrid reasoning frameworks combining deep learning with symbolic AI for scientific discovery. His research interests include AI for climate science, physics-informed neural networks, and interpretable machine learning for complex environmental systems.

PLACE PHOTO HERE

Cheikh Brahim EL VAIGH is an associate professor at Université Bourgogne Europe(France), CIAD. He is also a visiting researcher at the Osaka University Institute for Datability Science since 2019. He received his MASc degree in computer science from Université de Rennes (France) in 2017 and his Ph.D. in January 2021 from the same university. During his Ph.D., he worked on the joint use of knowledge graph and NLP for data-journalism at the INRIA/IRISA lab (Rennes, France). His research is focused on data analysis with join approaches leveraging knowledge graphs such as text and graph, or image and graph learning. He is also working on ontology mediated query answering querying with both RDF and description logics.

PLACE PHOTO HERE

Nicolas Gros is a research engineer at the CIAD Laboratory (University of Burgundy), where he has worked since 2018. He is in charge of research partnership development and technology transfer. He holds a Master of Science, Technology, and Health with a specialization in Computer Science and Artificial Intelligence, earned in 2017. His academic focus was on databases and artificial intelligence. At CIAD, he contributes to the promotion and valorization of research results and supports collaborative initiatives between academia and industry. He is actively involved in interdisciplinary projects that leverage AI technologies to address real-world challenges.

PLACE PHOTO HERE

Aurélie Bertaux born in 1978, is a Full Professor in Computer Science at Université Bourgogne Europe and Deputy Director of the CIAD laboratory (Connaissance et Intelligence Artificielle Distribuées) in Dijon, France. She defended her PhD in 2010 and became Associate Professor in 2013. In 2019, she obtained her Habilitation à Diriger des Recherches (HDR) with a thesis titled Toward Artificial Intuition. Her research lies at the intersection of artificial intelligence, data mining, machine learning, and formal concept analysis, with a strong focus on hybrid symbolic/sub-symbolic models and human-inspired reasoning. She actively supervises research projects and PhD theses in these areas, contributing to the development of interpretable, adaptive, and collaborative AI systems.

PLACE PHOTO HERE

Ouassila Labbani-Narsis is a Lecturer in Computer Science at the University of Burgundy since 2008 and a member of the CIAD Laboratory. She received her PhD in 2006 from the University of Science and Technology of Lille and completed a postdoctoral fellowship at ENS Lyon and INRIA Rhône-Alpes (2006–2008). She obtained her habilitation for supervising research in 2023. Her research focuses on hybrid and distributed artificial intelligence, knowledge and ontology engineering, model-driven engineering, and semantic constraint verification. She is actively involved in national and European research projects and has published numerous peer-reviewed papers in top-tier journals and international conferences in artificial intelligence, knowledge engineering, and semantic reasoning.

PLACE PHOTO HERE

SANDEEP KUMAR received the master's (Hons.) and Ph.D. degrees from South Asian University, New Delhi, India. His research interests include transfer learning, machine learning, and intrusion detection. He is an active member of IEEE Computational Intelligence Society. He is also an active reviewer in various journals, such as Heliyon, Applied Soft Computing, and Engineering Applications of Artificial Intelligence. He received the prestigious INSPIRE fellowship from the Department of Science and Technology, Government of India, during the Ph.D. degree.

PLACE PHOTO HERE

Gérard Colas des Francs received the M. Sc. degree from ENS Paris-Saclay, France in 1999 and PhD degree in Physics from University Toulouse, France, in 2002. After a Marie Curie postdoctoral fellowship at the University of Münster (Germany), he joined CNRS as a junior CNRS researcher at the Laboratoire Interdisciplinaire Carnot de Bourgogne (ICB), Dijon France in 2004. Since 2011, he has been a full professor at the University Bourgogne-Europe. His research interests include nano photonics, plasmonics, and quantum plasmonics.

PLACE PHOTO HERE

Alexandre Bouhelier is a CNRS Director of Research at the Laboratoire Interdisciplinaire Carnot de Bourgogne, Université de Bourgogne Europe. His work focuses on nanophotonics and plasmonics, bridging optoelectronics with nanoelectronics through novel memristive devices capable of light emission and detection. He also explores nonlinear plasmonics, particularly the dynamics of hot carriers and their role in frequency conversion and logic operations. With over 150 publications and more than 5,700 citations, Bouhelier has gathered international recognition from his peers. He has directed major technological platforms, coordinated multi-million-euro research projects, and contributed extensively to the development of advanced optical instrumentation. As deputy director of ICB, he supports strategic development, notably the i-NanoT initiative in theranostic nanovectors. A regular speaker at top-tier conferences, he also mentors PhD students and postdocs, advancing innovation at the intersection of light and matter.

PLACE PHOTO HERE

Christophe Nicolle is a professor of computer science at Université de Bourgogne and the founder of the CIAD Laboratory (Connaissance, Ingénierie et Aide à la Décision), a research center focused on artificial intelligence, knowledge engineering, and decision support systems. He co-founded Active3D in 2002, a company specializing in 3D digital twins for complex infrastructure management, now part of Sopra Steria. In 2019, he launched Wittym, a company that develops semantic and AI solutions to enhance knowledge representation and data interoperability. Nicolle also created the Checksem business unit, supporting companies in deploying trustworthy AI solutions. With a strong background in both academic and industrial R&D, he plays a key role in bridging scientific research and operational innovation. His work often combines distributed AI, ontologies, and human- centered system design, aiming to deliver robust, explainable, and useful AI systems for industry and public services.

PLACE PHOTO HERE

Erik Dujardin is a CNRS Research Director at ICB (CNRS UBE UMR 6303, Dijon, Fr). As a physical chemist, he has authored 110 publications in high impact international peer- reviewed journals, 4 book chapters gathering ¿ 15000 citations and given 40 invited conferences on carbon nanotubes, graphene, nanoplasmonics, nanowetting and bionanomaterials. In recent years, his main focus has been to introduce the concept of interconnect-free all-optical Boolean computing using 2-dimensional plasmonic cavities and he developed a new interdisciplinary approach to implement it that involves chemical synthesis, advanced nanofabrication steps and general nano-optical encoding/decoding of binary information. Besides, he is also innovating optically-active nanomaterials synthesis and assembly methods by creating a new concept of functional protein origami.